

Nonlinear Damping in Nanomechanical Beam Oscillator

Stav Zaitsev, *Student Member, IEEE*, Ronen Almog, Oleg Shtempluck and Eyal Buks

Abstract— We investigate the impact of nonlinear damping on the dynamics of a nanomechanical doubly clamped beam. The beam is driven into nonlinear regime and the response is measured by a displacement detector. For data analysis we introduce a nonlinear damping term to Duffing equation. The experiment shows conclusively that accounting for nonlinear damping effects is needed for correct modeling of the nanomechanical resonators under study.

Index Terms—Mechanical damping, nonlinear, bistability, NEMS, multiple scales.

I. INTRODUCTION

THE field of micro-machining is forcing a profound redefinition of the nature and attributes of electronic devices. This technology allows fabrication of a variety of on-chip fully integrated sensors and actuators with a rapidly growing range of applications. In many cases it is highly desirable to shrink the size of mechanical elements down to the nano-scale [1], [2]. This allows enhancing the speed of operation by increasing the frequencies of mechanical resonances and improving their sensitivity as sensors. Moreover, as devices become smaller, their power consumption goes down and their cost can be significantly lowered. Some key applications of nanoelectromechanical systems (NEMS) technology include magnetic resonance force microscopy (MRFM) [3], [4] and mass-sensing [5]. Further miniaturization is also motivated by the quest for mesoscopic quantum effects in mechanical systems [6], [7], [8].

A key property of systems based on mechanical oscillators is the rate of damping. For example, in many cases the sensitivity of NEMS sensors is limited by thermal fluctuation which is related to damping via the fluctuation dissipation theorem. In general, a variety of different physical mechanisms can contribute to damping, including bulk and surface defects, thermoelastic damping, nonlinear coupling to other modes, phonon-electron coupling, clamping loss etc. Identifying experimentally the contributing mechanisms in a given system can be highly challenging, as the dependence on a variety of parameters has to be examined systematically. Nanomechanical systems suffer from low quality factors Q relative to their macroscopic counterparts [2]. This behavior suggests that damping in nanomechanical devices is dominated by surface properties, since the relative number of atoms on the surface or close to the surface increases as device dimensions decrease. This point of view is also supported by some experiments [9], [10]. However, very little is currently

known about the underlying physical mechanisms contributing to damping in these devices.

In the present paper we study damping in a nanomechanical oscillator operated in the nonlinear regime. Nonlinear effects are of great importance for nanomechanical devices. The relatively small applied forces needed for driving a nanomechanical oscillator into the nonlinear regime is usually easily accessible. Thus, a variety of useful applications such as frequency synchronization, frequency mixing and conversion, parametric and intermodulation amplification [11], mechanical noise squeezing [12], and enhanced sensitivity mass detection [13] can be implemented by applying modest driving forces. Moreover, monitoring the displacement of a nanomechanical resonator oscillating in the linear regime may be difficult when a displacement detector with high sensitivity is not available. Thus, in many cases the nonlinear regime is the only useful regime of operation. However, to optimize the properties of NEMS devices operating in the nonlinear regime it is important to characterize the effect of damping in this regime.

The effect of nonlinear damping for the case of strictly dissipative force, being proportional to the velocity to the p 'th power, on the response and bifurcations of driven Duffing [14], [15], [16], [17] and other types of nonlinear oscillators [18], [19], [16] have been studied extensively. For the present case we consider a Duffing oscillator having nonlinear damping force proportional to the velocity cubed. As will be shown below, this approach is equivalent to the case where damping nonlinearity proportional to the velocity multiplied by the displacement squared is considered (see Ref. [20]). We have recently studied a closely related problem of a nonlinear stripline superconducting electromagnetic oscillator [21], [22], where nonlinear damping was taken into account. With some adjustments, these results are implemented for the case of a nanomechanical nonlinear oscillator. To determine experimentally the rate of nonlinear damping, as well as the Kerr constant and other important parameters, we measure the response near the resonance in the nonlinear regime [23], [24]. Measuring these parameters under varying conditions provides important insights into the underlying physical mechanisms.

II. EXPERIMENTAL SETUP

For the experiments we employ nanomechanical oscillators in the form of doubly clamped beams made of PdAu (see Fig. 1). The bulk nano-machining process used for sample fabrication is similar to the one described in Ref. [24]. The dimensions of the beams are length 100-200 μ m, width

0.25- μm and thickness 0.2 μm , and the gap separating the beam and the electrode is 5 μm . Measurements of mechanical properties are done *in-situ* a scanning electron microscope, where the imaging system of the microscope is employed for displacement detection [24]. Some of the samples were also measured using an optical displacement detection system described elsewhere [12]. Driving force is applied to the beam by applying a voltage to the nearby electrode. With a relatively modest driving force the system is driven into the region of nonlinear oscillations [24], [25].

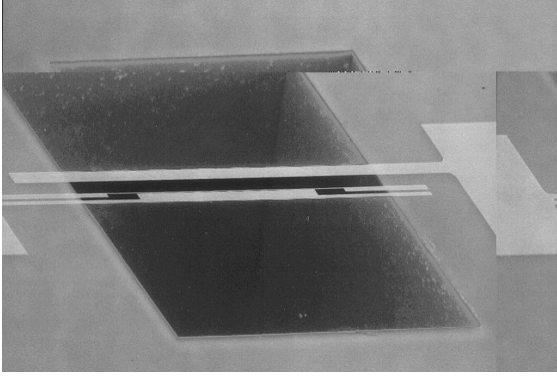


Fig. 1. The device consists of a narrow cantilever beam (length 200 μm , width 1-0.25 μm and thickness 0.2 μm) and wide electrode. The excitation force is applied as voltage between the beam and the electrode.

III. EQUATION OF MOTION

We excite the system close to its linear fundamental mode. Ignoring all higher modes allows us to describe the dynamics using a single degree of freedom x .

The nonlinear equation of motion is

$$m\ddot{x} + 2b_1\dot{x} + k_1x + b_3\dot{x}^3 + k_3x^3 = -\frac{d\mathcal{E}_{cap}}{dx}, \quad (1)$$

where m is the effective mass of the fundamental mode, $\mathcal{E}_{cap} = C(x)V^2/2$ is the capacitance energy, $C(x) = C_0/(1 - x/d)$ is the displacement dependent capacitance, d is the gap between the electrode and the beam, b_1 is the linear damping constant, b_3 is the nonlinear damping constant, k_1 is the linear spring constant and k_3 is the nonlinear (Kerr) spring constant.

The applied voltage is composed of large DC and small AC components $V(t) = V_{DC} + v \cos(\omega t)$ where v is constant and $v \ll V_{DC}$. Thus the equation of motion reads

$$(1 - x/d)^2(\ddot{x} + 2\gamma_1\dot{x} + \omega_0^2x + \gamma_3\dot{x}^3 + \alpha_3x^3) = F(1 + 2f \cos(\omega t)), \quad (2)$$

where $\omega_0 = \sqrt{k_1/m}$, $\gamma_1 = b_1/m = \omega_0/2Q$ (Q being the mechanical quality factor), $\gamma_3 = b_3/m$, $\alpha_3 = k_3/m$, $F = C_0V_{DC}^2/2md$ and $f = v/V_{DC}$.

IV. MULTIPLE SCALES APPROXIMATION

We use the standard multiple scales method to solve Eq. (2) [18], [26]. The harmonic excitation frequency is assumed to be close to the primary resonance

$$\omega = \omega_0 + \sigma,$$

where $\sigma \ll \omega_0$ is a small detuning parameter. We also assume the linear damping coefficient γ_1 , both coefficients of nonlinear terms, γ_3 , α_3 , and $1/d$ to be small. Keeping terms up to the first order in the small parameters leads to the following form of the solution for $x(t)$

$$x(t) = \frac{F}{\omega_0^2} + (A(t)e^{i\omega_0 t} + c.c.), \quad (3)$$

where the first term in the right-hand side is a constant displacement due to electrostatic attractive force, and $A(t)$ is slowly varying envelope (on the time scale of $1/\omega_0$). The differential equation for $A(t)$ in this approximation is given by

$$2\omega_0 \left[i \frac{dA}{dt} + (i\gamma_1 + \Delta\omega_0) A \right] + 3(\alpha_3 + i\gamma_3\omega_0^3) A^2 A^* = F f e^{i\sigma t}, \quad (4)$$

where $\Delta\omega_0 = (3\alpha_3 F/\omega_0^4 - 2/d) F/2\omega_0$ is a small correction to the linear resonance frequency ω_0 .

The solution for $A(t)$ can be represented as

$$A(t) = a e^{i(\phi + \Delta\omega_0 t)}, \quad (5)$$

where a and ϕ are real. Substituting Eq. (5) into Eq. (4) and separating real and imaginary parts one finds

$$-2\omega_0 a \frac{d\phi}{dt} + 3\alpha_3 a^3 = F f \cos(\phi - \Delta\omega t), \quad (6a)$$

$$-2\omega_0 \left(\frac{da}{dt} + \gamma_1 a \right) - 3\gamma_3 \omega_0^3 a^3 = F f \sin(\phi - \Delta\omega t), \quad (6b)$$

where $\Delta\omega = \sigma - \Delta\omega_0$ is the excitation frequency detuning from the shifted resonance frequency $\omega_0 + \Delta\omega_0$. In the steady state a and $\phi - \Delta\omega t$ are constant and the following equation for the steady state response amplitude a can be derived from Eq. (6)

$$9(\alpha_3^2 + \gamma_3^2 \omega_0^6) a^6 + 12\omega_0(\gamma_1 \gamma_3 \omega_0^3 - \Delta\omega \alpha_3) a^4 + 4\omega_0^2(\Delta\omega^2 + \gamma_1^2) a^2 - F^2 f^2 = 0, \quad (7)$$

Equation of the same form was obtained in Ref. [21], where a superconducting oscillator having Kerr nonlinearity in addition to nonlinear damping was considered. All subsequent analysis is thus based on Ref. [21].

When γ_3 is sufficiently small the solutions of Eq. (7) behave very much like the ordinary Duffing equation solutions to which Eq. (1) reduces to when $b_3 = 0$ (see Fig. 2).

Interestingly enough, equations similar to Eq. (4) and Eq. (7) arise when the damping nonlinearity is considered to be proportional to velocity multiplied by the displacement squared (instead of velocity cubed)

$$m\ddot{x} + 2b_1\dot{x} + k_1x + b_3x^2\dot{x} + k_3x^3 = -\frac{d\mathcal{E}_{cap}}{dx}.$$

Substituting γ_1 by $(\gamma_1 + \gamma_3 F^2/2\omega_0^4)$ and γ_3 by $\gamma_3(1 + 2F/\omega_0^2)/3\omega_0^2$ in Eq. (4) and Eq. (7) gives the correct relations for this case. Therefore, the behavior for these two cases is similar near the resonance frequency.

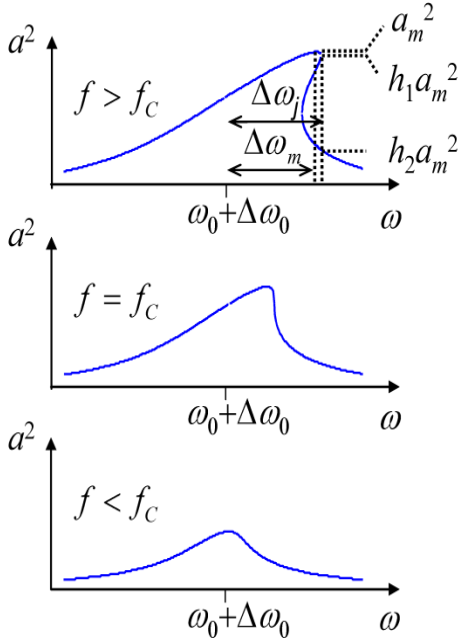


Fig. 2. Steady state solutions under different excitation amplitudes f . In case $f < f_c$ only one real solution exists, no bistability is possible. In case $f = f_c$ the system is on the edge of bistability, and one point exists where a^2 vs. ω has infinite slope. In case $f > f_c$ the system is in bistable regime having three real solutions over some range of frequencies. Two of these solutions are stable.

V. SPECIAL POINTS

Referring to Fig. 2 we define some points in the a^2 vs. ω curves which we use in experimental data analysis.

The first point is the maximum response, shifted by $\Delta\omega_m$ from $\omega_0 + \Delta\omega_0$ and having the amplitude a_m . Differentiating Eq. (7) with respect to $\Delta\omega$ and demanding $d(a^2)/d\Delta\omega = 0$ yields

$$a_m^2 = \frac{2\omega_0\Delta\omega_m}{3\alpha_3}. \quad (8)$$

Another point of special interest is the point where the jump in amplitude occurs and therefore the condition $d\Delta\omega/d(a^2) = 0$ must be satisfied. Applying this condition to Eq. (7) yields

$$27(\alpha_3^2 + \gamma_3^2\omega_0^6)a^4 + 24\omega_0(\gamma_1\gamma_3\omega_0^3 - \Delta\omega\alpha_3)a^2 + 4\omega_0^2(\Delta\omega^2 + \gamma_1^2) = 0. \quad (9)$$

Eq. (9) has a single real solution at the point of critical frequency $\Delta\omega_c$ and critical amplitude a_c , where the system is on the edge of bistability. This point is defined by two conditions

$$\begin{aligned} \frac{d\Delta\omega}{d(a^2)} &= 0, \\ \frac{d^2\Delta\omega}{d(a^2)^2} &= 0. \end{aligned}$$

In general, γ_3 is positive but α_3 can be either positive (hard spring) or negative (soft spring). In our experiment $\alpha_3 > 0$. By applying these conditions one finds

$$\Delta\omega_c = \frac{\gamma_1 p + 3}{\sqrt{3}1 - p}, \quad (11a)$$

$$a_c^2 = \frac{4}{3\sqrt{3}} \frac{\gamma_1\omega_0}{\alpha_3} \frac{1}{1 - p}, \quad (11b)$$

where $p = \sqrt{3}\gamma_3\omega_0^3/\alpha_3$. The driving force at this critical point is denoted in Fig. 2 as f_c . Note that bistable region is accessible only when $p < 1$.

VI. EXPERIMENTAL DATA AND RESULTS

A typical measured response of the fundamental mode of a $200\mu\text{m}$ ($125\mu\text{m}$) long beam occurring at $f_0 = 123.2\text{kHz}$ ($f_0 = 524.6\text{kHz}$) measured with $V_{DC} = 20\text{V}$ and varying excitation amplitude is seen in Fig. 3(a) (Fig. 3(b)). We derive the value of $\gamma_1 = \omega_0/2Q$ from the linear response at low excitation amplitude and find $Q = 7200$ ($Q = 2100$).

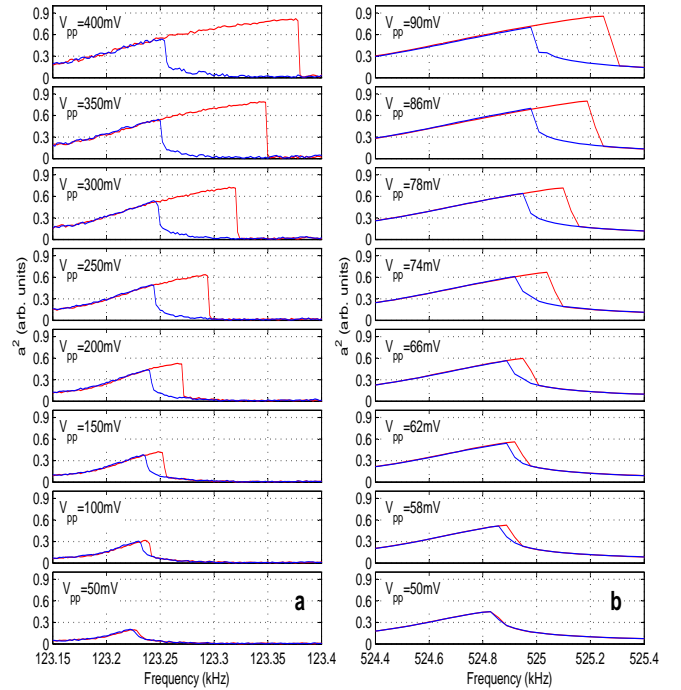


Fig. 3. Measured response vs. frequency shown for both upward and downward frequency sweeps with $V_{DC} = 20\text{V}$ and with varying peak-to-peak excitation amplitude V_{pp} . (a) $200\mu\text{m}$ long beam with fundamental mode occurring at $f_0 = 123.2\text{kHz}$. (b) $125\mu\text{m}$ long beam with fundamental mode occurring at $f_0 = 524.6\text{kHz}$.

Our displacement detector is highly nonlinear, introducing thus a significant distortion in the measured response. In order to minimize the resultant inaccuracies, we employ the following method to extract the nonlinear parameters.

In general, the sum of the three solutions for a^2 at any given frequency can be found from Eq. (7). This is employed for the jump point at $\omega_0 + \Delta\omega_j$ seen in Fig. 2. Using Eq. (8) to calibrate the measured response at this jump point one has

$$(2h_1 + h_2) \frac{2\omega_0\Delta\omega_m}{3\alpha_3} = - \frac{4\omega_0(\gamma_1\gamma_3\omega_0^3 - \Delta\omega_j\alpha_3)}{3(\alpha_3^2 + \gamma_3^2\omega_0^6)},$$

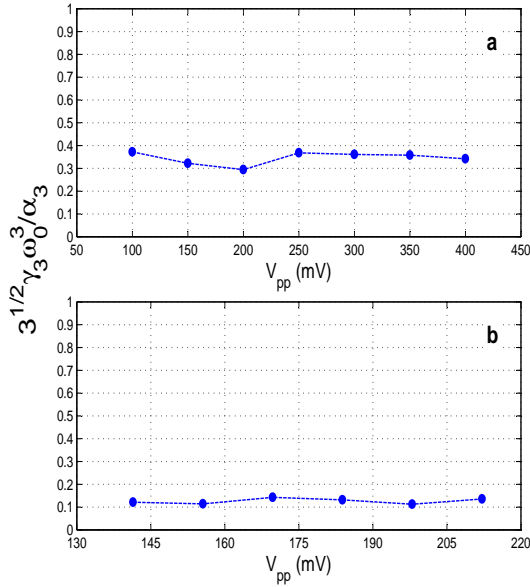


Fig. 4. Experimental results for $p = \sqrt{3}\gamma_3\omega_0^3/\alpha_3$ vs. peak-to-peak excitation amplitude V_{pp} . (a) 200 μm long beam with fundamental mode occurring at $f_0 = 123.2$ kHz and $Q = 7200$. (b) 125 μm long beam with fundamental mode occurring at $f_0 = 524.6$ kHz and $Q = 2100$.

or

$$(2h_1 + h_2) \Delta\omega_m \left(\frac{p^2}{3} + 1 \right) + 2 \left(\gamma_1 \frac{p}{\sqrt{3}} - \Delta\omega_j \right) = 0, \quad (13)$$

where h_1 and h_2 are defined in Fig. 2. Due to the frequency proximity between the maximum point and the jump point at $\omega = \omega_0 + \Delta\omega_j$ the inaccuracy of such a calibration is small. Moreover, as long as excitation amplitude is high enough, h_2 is much smaller than h_1 and even considerable inaccuracy in h_2 estimation will not have any significant impact. This equation can be used to estimate p for different excitation amplitudes. The results of applying Eq. (13) to experimental data from the two different beams can be seen in Fig. 4.

Using this procedure we find $p \approx 0.35$ for the 200 μm long beam and $p \approx 0.14$ for the 125 μm long beam. These results are identical to the values of p estimated using Eq. (11a). Referring to Eq. (11) and Eq. (9) we see that in our system the damping nonlinearity is not negligible and has a measurable impact on both the amplitude and frequency offset of the critical point, as well as on jump points in the bistable region.

To determine the value of α_3 we measure the static deflection of the beam's center as a function of an applied DC voltage V_{DC} . From a fit to theory we find $\alpha_3 = \omega_0^2 \cdot 0.092 \mu\text{m}^{-2}$ for the 200 μm long beam.

VII. CONCLUSIONS

In this work we have demonstrated conclusively that nonlinear damping in nanomechanical doubly-clamped beam oscillator may play an important role. The method presented in this paper may allow a systematic study of nonlinear damping in nano-mechanical oscillators, which may help revealing the underlying physical mechanisms.

ACKNOWLEDGMENT

We would like to thank B. Yurke, O. Gottlieb and R. Lifshitz for many fruitful discussions. This work was partially supported by Intel Corporation, US-Israel binational foundation and by the Israeli Ministry of Science.

REFERENCES

- [1] M. Roukes, "Nanoelectromechanical systems face the future," *Phys. World*, vol. 14, p. 25, Feb 2001.
- [2] —, "Nanomechanical systems," *Technical Digest of the 2000 Solid State Sensor and Actuator Workshop*, 2000.
- [3] J. A. Sidles, J. L. Garbini, K. J. Bruland, D. Rugar, O. Zuger, S. Hoehn, and C. S. Yannoni, "Magnetic resonance force microscopy," *Rev. Mod. Phys.*, vol. 67, no. 1, pp. 249–265, Jan 1995.
- [4] D. Rugar, R. Budakian, and H. J. M. an B. W. Chui, "Single spin detection by magnetic resonance force microscopy," *Nature*, vol. 430, pp. 329–332, Jul 2004.
- [5] K. L. Ekinci, Y. T. Yang, and M. L. Roukes, "Ultimate limits to inertial mass sensing based upon nanoelectromechanical systems," *J. Appl. Phys.*, vol. 95, no. 5, pp. 2682–2689, Mar 2004.
- [6] M. Blencowe, "Quantum electromechanical systems," *Phys. Rep.*, vol. 395, pp. 159–222, 2004.
- [7] R. G. Knobel and A. N. Cleland, "Nanometre-scale displacement sensing using a single electron transistor," *Nature*, vol. 424, pp. 291–293, Jul 2003.
- [8] M. D. LaHaye, O. Buu, B. Camarota, and K. C. Schwab, "Approaching the quantum limit of a nanomechanical resonator," *Science*, vol. 304, pp. 74–77, Apr 2004.
- [9] K. Y. Yasumura, T. D. Stowe, E. M. Chow, T. Pfafman, T. W. Kenny, B. C. Stipe, and D. Rugar, "Quality factors in micron- and submicron-thick cantilevers," *J. MEMS*, vol. 9, no. 1, pp. 117–125, Mar 2000.
- [10] T. Ono, D. F. Wang, and M. Esashi, "Time dependence of energy dissipation in resonating silicon cantilevers in ultrahigh vacuum," *Appl. Phys. Lett.*, vol. 83, no. 10, pp. 1950–1952, Sep 2003.
- [11] R. Almog, S. Zaitsev, O. Shtempluck, and E. Buks, "High intermodulation gain in a micromechanical duffing resonator," *Appl. Phys. Lett.*, vol. 88, no. 213509, May 2006.
- [12] —, "Noise squeezing in a nanomechanical duffing resonator," *arXiv:cond-mat*, no. 0607055, Jul 2006.
- [13] E. Buks and B. Yurke, "Mass detection with nonlinear nanomechanical resonator," *arXiv:quant-ph*, no. 0606081, Jun 2006.
- [14] B. Ravindra and A. K. Mallik, "Role of nonlinear dissipation in soft duffing oscillators," *Phys. Rev. E*, vol. 49, no. 6, pp. 4950–4954, Jun 1994.
- [15] —, "Stability analysis of a non-linearly damped duffing oscillator," *J. Sound Vib.*, vol. 171, no. 5, pp. 708–716, 1994.
- [16] J. L. Trueba, J. Rams, and M. A. F. Sanjuan, "Analytical estimates of the effect of nonlinear damping in some nonlinear oscillators," *Int. J. Bifurcation and Chaos*, vol. 10, no. 9, pp. 2257–2267, 2000.
- [17] J. P. Baltanas, J. L. Trueba, and M. A. F. Sanjuan, "Energy dissipation in a nonlinearly damped Duffing oscillator," *Physica D*, vol. 159, pp. 22–34, 2001.
- [18] A. H. Nayfeh and D. T. Mook, *Nonlinear Oscillations*, ser. Wiley Classics Library. New York: Wiley, 1995.
- [19] M. A. F. Sanjuan, "The effect of nonlinear damping on the universal escape oscillator," *Int. J. Bifurcation and Chaos*, vol. 9, no. 4, pp. 735–744, 1999.
- [20] R. Lifshitz and M. C. Cross, "Response of parametrically driven nonlinear coupled oscillators with application to micromechanical and nanomechanical resonator arrays," *Phys. Rev. B*, vol. 67, no. 134302, 2003.
- [21] B. Yurke and E. Buks, "Performance of cavity-parametric amplifiers, employing kerr nonlinearities, in the presence of two-photon loss," *arXiv:quant-ph*, no. 0505018, Nov 2005.
- [22] E. Buks and B. Yurke, "Dephasing due to intermode coupling in superconducting stripline resonators," *arXiv:quant-ph*, no. 0511033, Nov 2005.
- [23] E. Buks and M. L. Roukes, "Stiction, adhesion energy, and the Casimir effect in micromechanical systems," *Phys. Rev. B*, vol. 63, no. 033402, 2001.
- [24] —, "Metastability and the Casimir effect in micromechanical systems," *Europhys. Lett.*, vol. 54, no. 2, pp. 220–226, Apr 2001.
- [25] —, "Electrically tunable collective response in a coupled micromechanical array," *J. MEMS*, vol. 11, no. 6, pp. 802–807, Dec 2002.

- [26] A. H. Nayfeh, *Introduction to Perturbation Techniques*. New York: Wiley, 1981.